Journal of Materials Chemistry C

Accepted Manuscript

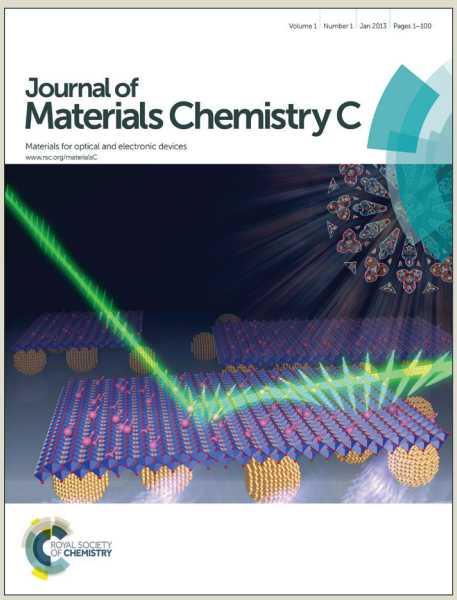

ROYAL SOCIETY OF CHEMISTRY

www.rsc.org/materialsC

Journal of Materials Chemistry C

COMMUNICATION

Super-stable Centimetre-scale Inverse Opal Belts Integrated with CdTe QDs for Narrow Band Fluorescence Optical Waveguiding

Received 00th January 20xx,
Accepted 00th January 20xx

DOI: 10.1039/x0xx00000x

www.rsc.org/

Xianyong Lu*[a], Lingmei Ni[a‖], Shimin Wu[a‖], Yanzi Wu[a], Hongyan Cai[a], Ke Ding[b], Lihong Jin[b], Yi Hou[b], Ying Zhu*[a], Mingyuan Gao[b] and Lei Jiang[ab]

Super-stable centimeter-scale SiO_2 inverse opal belts integrated with CdTe QDs have been prepared by synergetic collaboration among materials and structures. It can be found that SiO_2/CdTe inverse opal belts present excellent narrow band fluorescence optical waveguiding property.

Optical waveguide have been received great interest due to their potential applications in high speed data transmission of the next-generation processing system[1, 2]. As the performance of processors increases, a waveguide-based optical interconnects between processors, chips and even gates is becoming vital to the development of high performance digital systems[3,4]. Inverse opals with well-ordered periodic structures can provide an opportunity to manipulate photons within small volumes for photonic applications[5,6]. However, the optical properties of inverse opals are often limited by the relatively low refractive index of materials adopted such as silica[7]. In contrast, II-VI semiconductor materials have much higher refractive indices. Semiconductor nanomaterials such as nanowires, nanobelts have been reported to be used as optical integration devices, due to their 1D feature and advantageous photonic properties, such as optical waveguide and nanolaser source capabilities[8], which requires not only structurally stable waveguiding materials, but also effective coupling of photonic confinement of reverse opal structure and the electronic structure of the fluorescent semiconductor materials integrated, for achieving the high speed optical interconnect with large transmission distance. Nevertheless, the performance of absorption-emission-absorption of a waveguiding devices made up of semiconductors largely determines the loss of energy and the PL band structure of outlight[8,9]. Therefore, a rational integration of reverse opal structure with fluorescent semiconductors becomes essential for fulfilling the above-mentioned requirements. CdTe QDs are of high refractive index showing wide excitation spectra, high emission efficiency, electron transport efficiency, and excellent photochemical stability[10]. Doping fluorescent CdTe QDs in the colloidal crystals has been demonstrated to be an effective approach for coupling the fluorescent properties of QDs with the photonic confinement of the opal structures[11]. However, integrating CdTe QDs into an inverse opal structure to achieve waveguiding device with stable spontaneous emission is not reported yet.

In the current work, we report an easy and simple approach for fabricating centimeter-scale SiO_2/CdTe inverse opal belts showing highly reproducible spontaneous emission. The schematic illustration of preparation of SiO_2 inverse opal integrated with CdTe QDs is shown in Fig 1a. Firstly, centimetre-scale belts composed of cross-linked polyacrylic acid (c-PAA) colloidal particles were prepared via a curvature substrate and the negative pressure controlled vertical deposition (CSNPVD) method, as reported in our previous work[12]. PAA colloidal crystals were subsequently employed as a template for forming an inverse opal through a chemical vapour deposition (CVD) of tetraethoxysilane in a closed desiccator in the presence of ammonia[13]. Similar to a typical Stöber reaction, SiO_2 as infiltration material is formed by hydrolysis and condensation of tetraethoxysilane catalyzed by ammonia. A typical CVD was performed 24 hours, and PAA colloidal belts were coated by a uniform layer of silica shell. Then, SiO_2 inverse opal belts were obtained by removing the PAA colloidal crystal template under temperature of 600 °C in air atmosphere. Finally, SiO_2 inverse opal belts were immersed

[a] *Key Laboratory of Bio-Inspired Smart Interfacial Science and Technology of Ministry of Education, Beijing Key Laboratory of Bio-inspired Energy Materials and Devices, School of Chemistry and Environment, Beihang University, Beijing 100191, PR China*
[b] *Institute of Chemistry, Chinese Academy of Sciences, Beijing 100190, P. R. China*
† To whom correspondence should be addressed: (X.Lu) xylu@buaa.edu.cn, (Y. Zhu) zhuying@buaa.edu.cn
‖ These authors contributed equally to this work.
Electronic Supplementary Information (ESI) available: [details of any supplementary information available should be included here]. See DOI: 10.1039/x0xx00000x

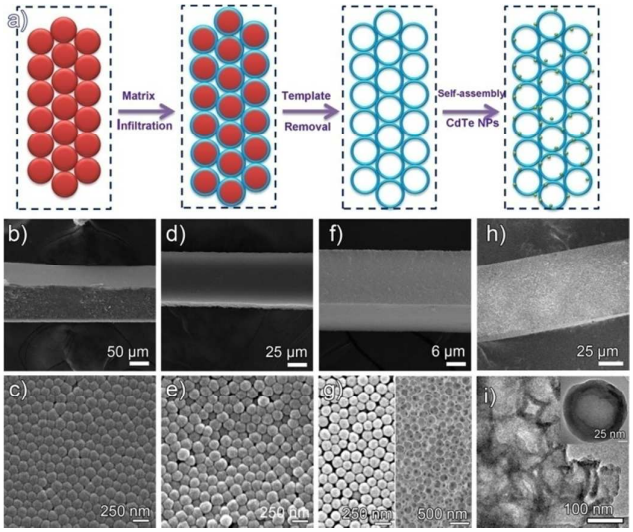

Fig 1. a) Schematic illustration of SiO_2 inverse opal belts integrated with CdTe QDs. b) and c) SEM images with different magnifications of PAA colloidal crystal belts. d) and e) PAA@SiO_2 colloidal crystal belts. f) and g) SiO_2 inverse opal belt. h), i)SEM image and cross-sectional TEM images taken from thin slices of silica inverse opals belt decorated with CdTe QDs, respectively.

into the thioglycolic acid(TGA)-capped CdTe QDs aqueous solution 8 hours[14], washed with water (pH=9.1) three times and vacuum dried. The shell thickness of SiO_2 inverse opal can be tuned by the duration of CVD. Subsequently, centimetre-scale SiO_2 inverse opal belts decorated with CdTe QDs exhibit a strong fluorescence emission under UV-vis irradiation. (seen supplementary information Fig S2).

The structures of PAA colloidal crystal belts, PAA@SiO_2 colloidal crystals belts, SiO_2 inverse opal belts and SiO_2 inverse opal belts integrated with CdTe QDs were characterized by scanning electron microscope (SEM) and transmission electron microscopy (TEM). The low-magnification SEM images shown in Fig. 1b-h indicate the internal structure changes in the process of forming SiO_2 inverse opal integrated with CdTe QDs. Fig. 1b and c are typical SEM images of PAA colloidal crystal belts which were obtained via a CSNPVD strategy. The average length of PAA colloidal belt is about 1 cm, which is composed of submicron c-PAA microspheres with average diameter of 159 ± 15 nm.[15] After CVD, the mean size of silica-coated c-PAA microspheres increased to 177 ± 14 nm. It is also clearly observed that silica-coated c-PAA microspheres provide more compact arrangement among submicrospheres than original c-PAA colloidal. After removing c-PAA materials, SiO_2 inverse opals are porous structures in which the pore arrangement is well ordered and interconnected without any cracks, as shown in Fig. 1g. The well-arranged porous, uniform silica wall and interconnected pore were contributed to the chemical vapour reaction, thus easily reaching the voids between c-PAA colloidal crystal (Fig. 1g).The thickness of silica wall is 18.0 ± 0.6 nm from a statics of SEM images. The interconnected porous structure (Fig. 1g), right image) shows that a majority

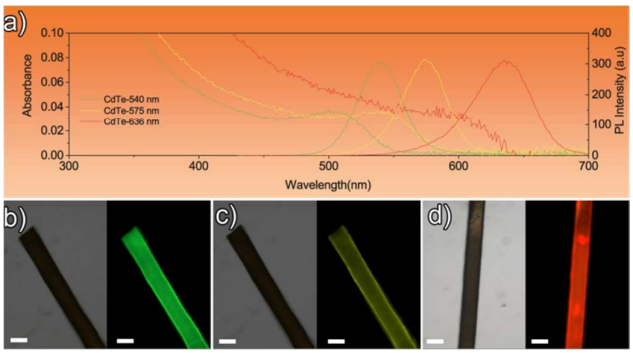

Fig 2. a) Absorption and PL spectra of the TGA-capped CdTe QDs with different size. The excitation wavelength for fluorescence measurements was 400 nm. Microscopic images of SiO2 inverse opal belts decorated with b) red emitting CdTe QDs, c)yellow-emitting CdTe QDs, d) red-emitting CdTe QDs, respectively . Photographs (all left images in b), c) d)) are bright-field images, whereas photographs (all left images in b), c) d)) are fluorescence images. The scale bars in the bright-field images correspond to 200 μm.

of connected points of the PAA colloids have connected pores. The average diameter of pores on the hollow SiO_2 microspheres is 55.2 ± 8.6 nm. When SiO_2 inverse opal belts were immersed in CdTe QDs colloid solution, CdTe QDs were introduced into the voids by capillary force[16,17]. The cross-sectional TEM images taken from thin slices of SiO_2 inverse opals decorated with CdTe QDs show that QDs were coated with the surface of SiO_2 hollow spheres. (Fig. 1i)) The optical properties of SiO_2 inverse opal belts integrated with CdTe QDs could be tuned by the size of CdTe nanocrystals, because CdTe QD nanocrystal have a strong size-dependent optical property[18]. Herein, there differently sized TGA-capped CdTe QDs with central photoluminescence peaking at 540 nm (green CdTe QDs), 575 nm (yellow CdTe QDs) and 636 nm (red CdTe QDs) were employed as for decorate SiO_2 inverse opal belts, respectively. Both fluorescence and absorption spectra of these three samples were shown in Fig. 2a. Due to the interconnected pores in SiO_2 inverse opal, there are strong capillary force between the CdTe QDs solution and inverse opal. Therefore, CdTe QDs were easily introduced into pores of SiO_2 inverse opal belts. SiO_2 inverse opal belts integrated with three differently sized CdTe QDs were also characterized by conventional fluorescence microscopy. The results shown in Fig. 2b-d prove that CdTe QDs have successfully decorated on the inner wall of porous SiO_2 microspheres which present a perfect one-to-one correspondence between the bright-field image and the fluorescence image.

Each TGA molecule bears two functional groups, i.e., mercapto group and carboxyl group. The mercapto group is bound on the surface of CdTe QDs[19], while the pendant carboxyl group provides not only aqueous solubility, but the possibility for coupling CdTe QDs with matrix materials (Fig. 3 b). SiO_2 hollow submicrospheres have a large number of hydroxyl groups. Therefore, CdTe QDs were expected to have strong interaction with SiO_2 inverse opal via hydrogen bonding interaction (shown in Fig 3 b)[20]. This interaction is based on

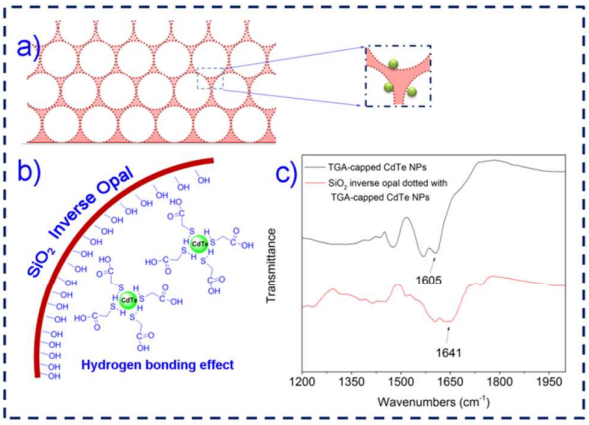

Fig 3. a)Schematic detail illustration of SiO_2 inverse opal dotted with CdTe QDs. b)the hydrogen bonding effect between SiO_2 hollow microsphere and TGA-capped CdTe QDs. c)FT-IR spectra of TGA-capped CdTe NPs (black line) and SiO_2 inverse opal dotted with TGA-capped CdTe NPs (red line).

hydroxyl group from SiO_2 inverse opal and carboxyl group on surface of TGA-capped CdTe QDs. This type of hydrogen bonding interaction was well characterized by FT-IR spectra (Fig. 3c). The peak located at 1605 cm^{-1} can be contributed to the stretching vibrations of the carbonyl group (C=O) of TGA-capped CdTe QDs[21]. However, when the CdTe QDs were decorated on the surface of SiO_2 inverse opal, the carbonyl group absorbing peak had 36 cm^{-1} red shift. These results indicated that there exist strong interactions between hydroxyl group and carbonyl group as hydrogen bonding[22], which enables the firm attachment of CdTe QDs on the surface SiO_2 inverse opal. It should be mentioned that SiO_2 inverse opal belts dotted with CdTe QDs are very stable under ambient conditions and remain fluorescently stable over 2 years(seen Fig S3 of supplementary information.).

The optical waveguide properties of the as-prepared SiO_2 inverse opal belts decorated with red CdTe QDs as a typical sample were studied using near-field scanning optical microscopy (NSOM), as schematically shown in Fig. 4a. When a SiO_2 inverse opal belt decorated with CdTe QDs was excited with a focused laser (λ = 405 nm) at the centre, fluorescence could be observed at end. Generally, light emission can only observed at the local area of the excited point in micro-area of fluorescence images[23]. The spectra of out light at end of SiO_2 inverse belts integrated with CdTe QDs suggests that this belts absorbs the excitation light and propagates the photoluminescence (PL) emission toward the end without light scattering at the edge of belts. It is a typical optical waveguide phenomenon. In order to gain further insights into the optical waveguiding behavior within 3D nanocomposite inverse opal belts, the spatially resolved near-field spectra of the propagation light at the output light point (Fig. 4c). The PL spectra of pure TGA-capped CdTe QDs is also located at 636 nm with the full width at half maximum (FWHM) 54.1 nm. In contrast, the SiO_2 inverse opal belts integrated with CdTe QDs revealed a decreasing of FWHM (10.4 nm) of the PL spectrum

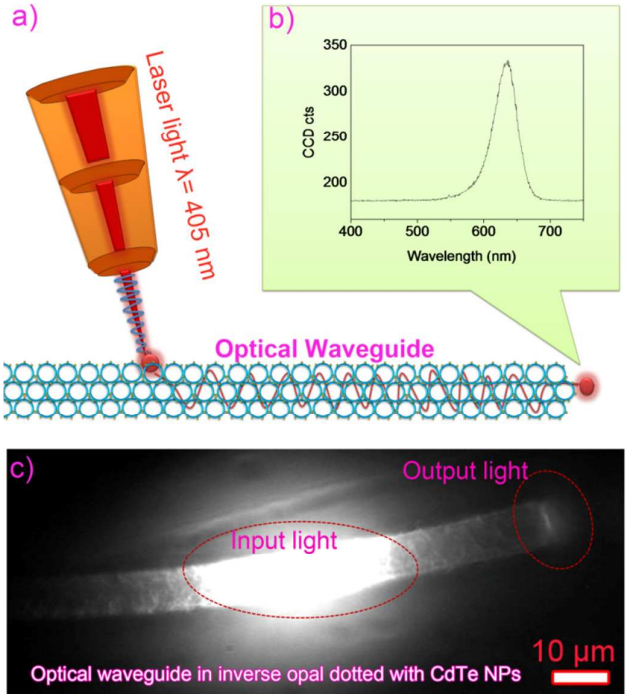

Fig 4. a) Schematic illustration of optical waveguiding in SiO_2 inverse opal belts decorated by CdTe QDs. b) PL spectra detected with the NSOM collection tip held at the terminus of nanocomposite inverse opal belts and with the excitation laser beam at side with angle of 45°. c) optical waveguiding in inverse opal belts detected with NSOM.

of output light. It indicates that the light propagates in the belts with stable PL band in SiO_2/CdTe inverse opal belts. The PL band with narrow FWHM the inverse opal structure plays an important role in integrating the PL band of CdTe QDs. Only the terminal of SiO_2/CdTe inverse opal belt in the same direction of light has output light from the image of NSOW, which proved that the photon was confined into the inverse opal belts during light propagation. SiO_2 inverse opal belts with other size CdTe QDs were also studied in Fig S4 of supplementary information. From above-mentioned results, SiO_2 inverse opal belts integrated with CdTe QDs exhibit excellent stable and narrow PL band in output light during light waveguiding .

Conclusions

In summary, we have successfully prepared super-stable centimetre-scale SiO_2 inverse opal belts integrated with CdTe QDs via hydrogen bonding interaction between carboxyl group of TGA and hydroxyl group of silica. SiO_2 inverse opal belts integrated with CdTe QDs serve as directional optical waveguide material excellent stable and significantly narrow PL band in output light. The new type optical waveguide materials have potential applications in a novel optical interconnect with controlling electrical and phonic confines.

Acknowledgments

The authors thank the financial support the Beijing Natural Science Foundation (2132030), the National Natural Science Foundation of China (21103006), China Scholarship Council (201303070263), 863 Program (2012AA030305), the Fundamental Research Funds for the Central Universities (YWF-10-01-B16, YWF-13-DX-XYJL-004).The authors thank Prof. Dr. Jin Zhai and Dr K. Wang their kind help on NSOW characterization.

Notes and references

1. L. Tong, R. R. Gattass, J. B. Ashcom, S. He, J. Lou, M. Shen, I. Maxwell and E. Mazur, Nature, 2003, 426, 816-819.
2. W. Hu, Y. Chen, H. Jiang, J. Li, G. Zou, Q. Zhang, D. Zhang, P. Wang and H. Ming, Adv. Mater., 2014, 26, 3136-3141.
3. X. Tong, in Advanced Materials for Integrated Optical Waveguides, Springer International Publishing, 2014, vol. 46, ch. 12, pp. 509-543.
4. S. K. Park, J.-M. Lee, S. Park, J. T. Kim, M.-s. Kim, M.-H. Lee and J. J. Ju, J. Mater. Chem., 2011, 21, 1755-1761.
5. A. Stein, B. E. Wilson and S. G. Rudisill, Chem. Soc. Rev., 2013, 42, 2763-2803.
6. J. Cui, W. Zhu, N. Gao, J. Li, H. Yang, Y. Jiang, P. Seidel, B. J. Ravoo and G. Li, Angew. Chem. Int. Ed., 2014, 53, 3844-3848.
7. V. L. Colvin, MRS Bull., 2001, 26, 637-641.
8. A. Pan, D. Liu, R. Liu, F. Wang, X. Zhu and B. Zou, Small, 2005, 1, 980-983.
9. J. Li, C. Meng, Y. Liu, X. Wu, Y. Lu, Y. Ye, L. Dai, L. Tong, X. Liu and Q. Yang, Adv. Mater., 2013, 25, 833-837.
10. Y. Li, L. Jing, R. Qiao and M. Gao, Chem. Commun., 2011, 47, 9293-9311.
11. D. Wang, A. L. Rogach and F. Caruso, Chem. Mater., 2003, 15, 2724-2729.
12. X. Y. Lu, Y. Zhu, T. Z. Cen and L. Jiang, Langmuir, 2012, 28, 9341-9346.
13. X. Deng, L. Mammen, H.-J. Butt and D. Vollmer, Science, 2012, 335, 67-70.
14. S. L. Wu, J. Dou, J. Zhang and S. F. Zhang, J. Mater. Chem., 2012, 22, 14573-14578.
15. F. Bai, X. L. Yang, R. Li, B. Huang and W. Q. Huang, Polymer, 2006, 47, 5775-5784.
16. J. P. Ge and Y. D. Yin, Angew. Chem. Int. Ed., 2011, 50, 1492-1522.
17. Y. Zhao, L. Shang, Y. Cheng and Z. Gu, Acc. Chem. Res., 2014, 47, 3632-3642.
18. A. J. Nozik, M. C. Beard, J. M. Luther, M. Law, R. J. Ellingson and J. C. Johnson, Chem. Rev., 2010, 110, 6873-6890.
19. A. A. Yaroslavov, V. A. Sinani, A. A. Efimova, E. G. Yaroslavova, A. A. Rakhnyanskaya, Y. A. Ermakov and N. A. Kotov, J. Am. Chem. Soc., 2005, 127, 7322-7323.
20. J. P. M. Lommerse, S. L. Price and R. Taylor, J. Comput. Chem., 1997, 18, 757-774.
21 H. Jiang and H. Ju, Anal. Chem., 2007, 79, 6690-6696.
22. G. R. Bardajee and Z. Hooshyar, J. Chem., 2013, DOI: 10.1155/2013/202061, 6.
23. L. Heng, X. Wang, D. Tian, J. Zhai, B. Tang and L. Jiang, Adv. Mater., 2010, 22, 4716-4720.

Graphic abstract

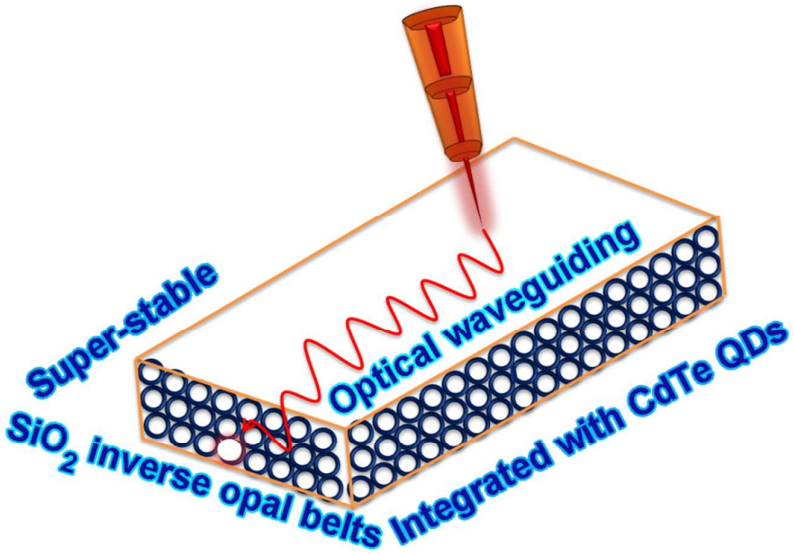

Structurally superstable centimeter-scale SiO_2 inverse opal belts integrated with CdTe QDs with excellent on-off optical waveguiding property.